ADVANCED FUNCTIONAL MATERIALS
www.afm-journal.de

Materials Views
www.MaterialsViews.com

Quasi-One Dimensional in-Plane Conductivity in Filamentary Films of PEDOT:PSS

*Kevin van de Ruit, Racheli Itzhak Cohen, Dirk Bollen, Ton van Mol, Rachel Yerushalmi-Rozen, René A. J. Janssen, and Martijn Kemerink**

The mechanism and magnitude of the in-plane conductivity of poly(3,4-ethylenedioxythiophene):poly(styrenesulfonate) (PEDOT:PSS) thin films is determined using temperature dependent conductivity measurements for various PEDOT:PSS weight ratios with and without a high boiling solvent (HBS). Without the HBS the in-plane conductivity of PEDOT:PSS is lower and for all studied weight ratios well described by the relation $\sigma = \sigma_0 \exp[-(\frac{T_0}{T})^{0.5}]$ with T_0 a characteristic temperature. The exponent 0.5 indicates quasi-one dimensional (quasi-1D) variable range hopping (VRH). The conductivity prefactor σ_0 varies over three orders of magnitudes and follows a power law $\sigma_0 \propto c^{3.5}_{PEDOT}$ with c_{PEDOT} the weight fraction of PEDOT in PEDOT:PSS. The field dependent conductivity is consistent with quasi-1D VRH. Combined, these observations suggest that conductance takes place via a percolating network of quasi-1D filaments. Using transmission electron microscopy (TEM) filamentary structures are observed in vitrified dispersions and dried films. For PEDOT:PSS films with HBS, the conductivity also exhibits quasi-1D VRH behavior when the temperature is less than 200 K. The low characteristic temperature T_0 indicates that HBS-treated films are close to the critical regime between a metal and an insulator. In this case, the conductivity prefactor scales linearly with c_{PEDOT}, indicating the conduction is no longer limited by a percolation of filaments. The lack of observable changes in TEM upon processing with the HBS suggests that the changes in conductivity are due to a smaller spread in the conductivities of individual filaments, or a higher probability for neighboring filaments to be connected rather than being caused by major morphological modification of the material.

1. Introduction

Practical interest in poly(3,4-ethylenedioxythiophene):poly(styrenesulfonate) (PEDOT:PSS), shown in **Figure 1**, is mainly driven by its widespread application as solution processable electrode layer in organic light emitting diodes and in organic and hybrid photovoltaic cells. In particular, these applications require a transparent conducting electrode which is generally provided by a layer of tin-doped indium oxide (ITO). Significant recent progress with respect to the combination of conductivity and transparency of PEDOT:PSS strongly indicates that it may be possible to replace the expensive and brittle ITO layer with a PEDOT:PSS layer.[1,2]

Additionally, PEDOT:PSS and other PEDOT-based systems exhibit several technologically relevant characteristics, such as charge transport properties in the critical regime close to the metal-insulator transition,[3–7] order of magnitude in-/out-of-plane anisotropy in the electrical conductivity,[8–10] power law behavior for the out-of-plane conductivity,[11,12] high thermoelectric figure of merit,[13] reversible volume changes,[14] and the existence of polarons or bipolarons depending on interchain interaction.[5,15]

To obtain PEDOT:PSS, the conductive element, PEDOT, which is undoped and insoluble in its pristine state is synthesized from 3,4-ethylenedioxythiophene (EDOT) in an aqueous solution containing the polyelectrolyte PSS. The PEDOT oligomers are attached to PSS chains by ionic interactions, which stabilize the doping of the PEDOT and solubilize the otherwise insoluble PEDOT in water, probably via the formation of core–shell micelles with a PEDOT-rich core and a PSS-rich shell.[16,17] Atomic force microscopy (AFM), scanning tunneling microscopy (STM), and transmission electron microscopy (TEM) studies indicate that these micelles are present in spin coated layers.[8,18,19] The morphology of the resulting layers is further complicated by the presence of composition gradients[20] or the presence of a lamellar structure.[8,21] Post-processing treatments of PEDOT:PSS thin films, aimed at improving the electro-optical properties of the film, are often thought to affect this morphology.[2,15,19,22–26]

K. van de Ruit, Prof. R. A. J. Janssen, Dr. M. Kemerink
Eindhoven University of Technology
Department of Applied Physics
P.O. Box 513, 5600 MB Eindhoven, The Netherlands
E-mail: m.kemerink@tue.nl
R. I. Cohen, Prof. R. Yerushalmi–Rozen
Department of Chemical Engineering
Ben-Gurion University of the Negev
Beer-Sheva 84105, Israel
D. Bollen
Agfa-Gevaert N.V, Septestraat 27, 2640 Mortsel, Belgium
Dr. A. M. B. van Mol
Holst Centre/TNO, High Tech Campus 48, 5656 AE Eindhoven
The Netherlands
Prof. R. Yerushalmi-Rozen
Ilze Kats Institute for Nanoscale Science and Technology
Ben-Gurion University of the Negev
Beer-Sheva 84105, Israel

DOI: 10.1002/adfm.201301174

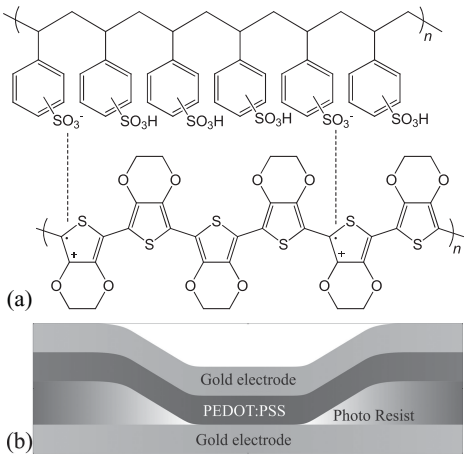

Figure 1. a) PEDOT (below) and PSS (top) are bound via the Coulomb attraction between charged monomers of both molecules, indicated by the dotted lines. b) Schematic representation of PEDOT:PSS.

Charge transport measurements are an important tool for gaining insight into the complex properties of PEDOT:PSS. Typically the temperature dependence of the conductivity is large and interpreted in the context of variable range hopping (VRH).[7–9,15,19,25,27] For the temperature dependent conductivity, $\sigma(T)$ at low bias, i.e., the Ohmic conductivity, VRH predicts that

$$\sigma(T) = \sigma_0 \exp\left[-\left(\frac{T_0}{T}\right)^{\alpha}\right] \quad (1)$$

where σ_0 is the conductivity prefactor, T_0 the characteristic temperature, and α a characteristic exponent related to the dimensionality of the system, d, by $\alpha = (1 + d)^{-1}$. VRH behavior has been measured in PEDOT:PSS with $\alpha = 1/2$ in spin-cast[2,15,19,22,25] and drop-cast[6,26,28] films and in nanowires,[4,27] with $\alpha \approx 1/3$ in drop-cast films[7] and with $\alpha = 1/4$ in spin-cast films.[8,9] With few exceptions[4,28] it was concluded that VRH correctly describes the mechanism of conduction. There is a remarkable high number of observations of quasi-one dimensional (quasi-1D) VRH in PEDOT:PSS. In some cases this could be directly related to morphology.[19,27] Other articles[2,6,15,22] cite the explanation of Epstein,[29] which describes a VRH system where states are weakly localized along the polymer backbone and strongly localized perpendicular to the backbone. Although such mechanism was shown to take place in cross-linked polyaniline,[29] it seems at odds with the granular morphology that is often observed in PEDOT:PSS films. Moreover, the prediction[29] that the electric field dependence of the conductivity relative to the Ohmic conductivity should not depend on temperature is inconsistent with the model suggested by Nardes et al.[19]

Here we explore the transport properties of PEDOT:PSS by characterizing the dependence of the conductivity on the composition (PEDOT to PSS ratio) and the temperature. The physical picture obtained from combining the two is more complex than expected. We find that the transport properties are best explained by VRH conduction through a percolating network of 1D filaments that is close to the percolation threshold. The combination of the two mechanisms offers a consistent explanation for the quasi-1D VRH behavior observed in many PEDOT:PSS systems. This mechanism is also consistent with the morphological features observed by TEM at cryogenic temperatures: we find that elongated filaments are already present in the dispersion, and maintain their presence in the dried layer, while their diameter shrinks. We extend our investigation to the more practically relevant PEDOT:PSS processed with a high boiling solvent (HBS) additive, which exhibits orders of magnitude higher conductivity. The linear relation between conductivity and PEDOT:PSS ratio indicates a network with higher connectivity far away from the percolation threshold.

2. Results and Discussion

In-plane conductivities were measured on thin spin cast films on glass substrates under high vacuum conditions. **Figure 2** shows the measured conductivity as a function of temperature and bias for native processed, i.e., processed without additives, PEDOT:PSS in the weight ratios of 1:2.5, 1:6, 1:12, and 1:20. Notice that for lower PEDOT:PSS ratios the range in conductivity shifts down and extends. This way, two features are clearly observed. First, the room temperature conductivity decreases significantly as the weight fraction of PSS increases while the temperature dependence of the Ohmic conductivity (at $F = 0$, i.e., zero electric field) increases. In particular, while a two orders of magnitude increase in the in-plane conductivity is observed for samples comprising 1:2.5 PEDOT to PSS (Figure 2a) when the temperature is raised from 10 to 275 K, a four order of magnitude increase in the conductivity is observed for the 1:20 samples (Figure 2d). Second, as the electric field is increased, especially the low temperature conductivity becomes higher and the temperature dependence of the in-plane conductivity becomes less.

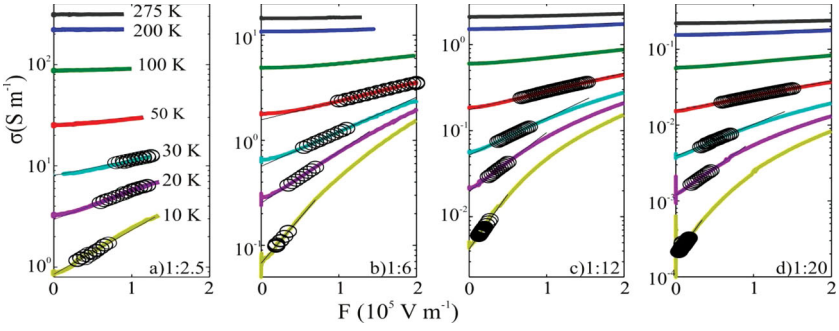

Figure 2. Solid lines are measurements of the in-plane conductivity vs. electric field at the indicated temperature for native PEDOT:PSS in the ratios: a) 1:2.5, b) 1:6, c) 1:12, and d) 1:20. The thin black lines indicate fits to the measurement points highlighted by the circular markers. Intermediate temperatures are not shown for clarity.

For all samples, finite electric fields have a similar effect as increased temperatures; hence the temperature dependence at large electric fields becomes reduced. This behavior is typical for doped disordered semiconductors such as PEDOT:PSS. In these materials,

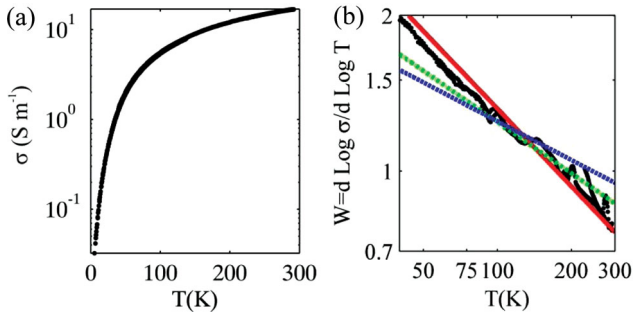

Figure 3. Measured a) Ohmic in-plane conductivities vs. temperature in a semi-logarithmic plot and the b) reduced activation energy W vs. temperature for native processed PEDOT:PSS in the ratio 1:6 in a double-logarithmic plot. The red, green and blue lines indicate slopes of 1/2, 1/3 and 1/4, resp. The black lines are double lines since the conductivity was measured while cooling down and while heating up.

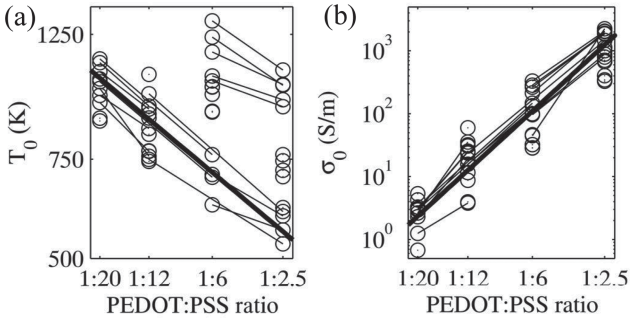

Figure 4. a) Characteristic temperatures and b) conductivity prefactors obtained from fits to the measured Ohmic conductivity vs. temperature for five spin coated samples of each of the four PEDOT:PSS ratios, prepared from two batches of newly prepared dispersions. Simultaneously measured data are connected by thin lines. Both panels are double-logarithmic plots with the x-axis scaled as the PEDOT concentration. The thick black lines indicate a slope of a) −0.35 and b) 3.5.

charge carriers move between localized states, or sites, by a thermally activated tunneling (i.e., hopping) process. As both thermal energy (k_BT) and an electric field in the hopping direction may provide the required energy for overcoming the energy difference between sites, a higher conductivity is reached when increasing the electric field or raising the temperature.

2.1. Composition Dependence of the Ohmic Conductivity in PEDOT:PSS

Figure 3 shows the Ohmic conductivity (i.e., at $F = 0$) and the reduced activation energy $W = d\ (\log\sigma)/d(\log T)$ for the (1:6) PEDOT:PSS (Figure 2). Graphs for the other ratios are shown in the Supporting Information, Figure S1. Fits to Mott's VRH theory (Equation (1)) are shown for $\alpha = 1/2$ (1D), 1/3 (2D), and 1/4 (3D) in red, green, and blue respectively. All PEDOT:PSS samples are best described by the characteristic exponent $\alpha = 1/2$, indicating that the in-plane transport in our samples is quasi-1D. The fitted parameters corresponding to $\alpha = 1/2$ are shown in **Table 1**. A truly one dimensional system of disordered wires of infinite length cannot conduct current because it will always contain a blocking site.[30] However, a large set of parallel one-dimensional conduction paths, or 'filaments' was shown to give rise to $\alpha = 1/2$.[31–33] For a particular PEDOT:PSS system processed with a high-boiling solvent morphological evidence was previously found to support such an interpretation.[19] A requirement[34] for the application of VRH theory is that $(T_0/T) >> 1$. For the native processed PEDOT:PSS and temperature range studied in this paper $(T_0/T) = 4–16$, which is in agreement with observations of other quasi-1D VRH systems.[4,27,35–37] A more detailed investigation of α yields that the data is best described by $\alpha = 0.45 \pm 0.05$, where α decreases slightly with temperature.

Table 1. Quasi-1D VRH fitting parameters for the different samples produced from the various PEDOT:PSS formulations, among which the samples discussed in Figures 3 and 8.

Samples	T_0 [K]	σ_0 [S m^{-1}]	σ (300 K) [S m^{-1}]
PEDOT:PSS, ratio 1:2.5	1.0×10^3	1.8×10^3	2.9×10^2
PEDOT:PSS, ratio 1:6	7.0×10^2	78	17
PEDOT:PSS, ratio 1:12	9.3×10^2	16	2.7
PEDOT:PSS, ratio 1:20	1.1×10^3	2.7	0.39
PEDOT:PSS, ratio 1:2.5 w/HBS	39	6.3×10^4	4.4×10^4
PEDOT:PSS, ratio 1:6 w/HBS	41	3.1×10^4	2.2×10^4
PEDOT:PSS, ratio 1:12 w/HBS	57	1.5×10^4	9.4×10^3
PEDOT:PSS, ratio 1:20 w/HBS	66	8.7×10^3	5.5×10^3

Alternative models found in literature which yield Equation (1) with $\alpha = 1/2$ can be excluded for the measurements discussed here. These are (*i*) Efros-Shlovskii VRH, which yields much bigger values of T_0,[38] and (*ii*,*iii*) Sheng et al.[38,39] and Zuppiroli et al.,[38,40] which contrary to quasi-1D VRH do not make testable predictions for low-field non-Ohmic behavior and which require the PEDOT:PSS ratio to be highly constant on a local scale, which is unlikely.

Figure 4 shows the characteristic temperatures T_0 and conductivity prefactors σ_0 obtained for five spin coated samples of each of the four PEDOT:PSS ratios, taken from two batches of newly prepared dispersions. To study the trend in σ_0 and T_0 with PEDOT concentration, connections between measurements points have been added to both Figure 4a,b. These connections indicate measurements that have been performed simultaneously. The data clearly show a decreasing characteristic temperature with increasing PEDOT concentration, which can be described using the empirical relation $T_0 \propto c_{\mathrm{PEDOT}}^{-0.35}$ indicated by the black line, where c_{PEDOT} is the weight fraction of PEDOT in PEDOT:PSS.

The values of the conductivity prefactor presented in Figure 4b show that reducing the concentration of the conductive polymer PEDOT by adding additional PSS strongly reduces the conductivity. The relation between conductivity and PEDOT concentration can be described by a power law: $\sigma_0 \propto c_{\mathrm{PEDOT}}^{3.5}$ indicated by the black line in Figure 4b. A similar power law dependence has been obtained when high aspect ratio conductive filaments were added to an insulating matrix.[41] This

behavior can be explained on basis of percolation theory: as conductive elements (PEDOT) are added to the insulating filler (PSS), conduction can occur when a path is formed by connected conductive elements, running from one electrode to the other. The lowest concentration at which this occurs is defined as the percolation threshold. Above this concentration the number of conduction paths strongly increases with increasing concentration of conductive material, typically causing the conduction to increase as a power law.[41] No threshold can be distinguished in Figure 4b. The conductive elements might at most contain PEDOT:PSS in a 1:2.5 ratio, otherwise the power law behavior would not persist up to 1:2.5. Assuming, as an upper limit, that the percolating filaments consist of PEDOT:PSS in a ratio 1:2.5 the volume fraction of percolating elements in the 1:20 material becomes (1:20):(1:2.5) = 12.5 vol%. Hence, the percolation threshold is much lower than 12.5 vol%, otherwise PEDOT:PSS in the ratio 1:20 would not show any conduction. The percolation threshold is known to depend on the dimensionality of the system and the geometry of the conducting objects. For a 3D system of spheres it is 29 vol%,[42] for disks,[43] and filaments[44] with a high aspect ratio (height to radius) it is much lower. Therefore, the percolation threshold being significantly below 12.5 vol% is consistent with a non-spherical shape of the conductive elements in PEDOT:PSS mixtures.

2.2. TEM Investigation

The microscopic morphology of PEDOT:PSS blends in dispersions and thin films has been investigated. TEM images of vitrified dispersions (cryo-TEM) and dried layers (HRTEM) of PEDOT:PSS samples are dominated by the presence of randomly oriented worm-like filaments, see **Figure 5**a,b. The cryo-TEM images indicate that the filament-like structures are already present in the dispersion and remain present in the dried layer, at a much higher concentration and reduced diameter. Similar images were obtained for PEDOT:PSS samples comprising a 1:20 ratio, see Supporting Information. PEDOT-rich grains with a PSS-rich shell were observed before in dried layers,[8,9,17,19,20,45,46] and via dynamic light scattering in dispersion.[46] We propose that the filaments observed in Figure 5a,b are similar structures, i.e., the filaments consist of a PEDOT-rich core and a PSS-rich shell. The filamentary structure of the films and the high aspect ratio of the observed filaments is fully consistent with the percolation behavior reflected in the power law dependence of the in-plane conductivity prefactor on PEDOT concentration (Figure 4b).

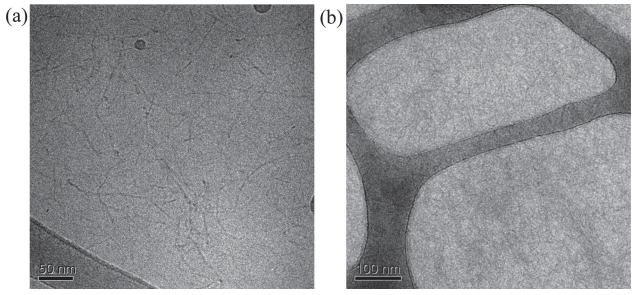

Figure 5. a) Cryo TEM image of PEDOT:PSS dispersion in the ratio 1:2.5. The darker areas are the TEM grid-lines. b) HRTEM image of dry specimen prepared from the same sample. The typical diameter of the filaments is 4-5 nm and their length may reach tens to hundreds of nanometers.

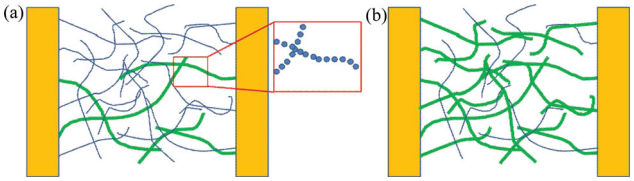

Figure 6. Schematic representation of filaments which determine the charge conduction in a) native processed PEDOT:PSS and b) PEDOT:PSS processed with HBS. The blue lines indicate the conducting filaments, of which the thick green lines show the filaments participating in the in-plane conduction. The yellow bars represent the electrodes. The red square indicates a zoom-in showing possible sites for charge carrier hopping along the chain. Compared to native processed PEDOT:PSS (a), the crossing points between filaments in PEDOT:PSS processed with HBS (b) have a much higher probability of being connected.

2.3. Consistent Description for the Composition Dependence of the Conductivity in the Native Processed Material

Based on the results presented in Figures 2–4, we propose the following hierarchical model for the in-plane conduction behavior of the present PEDOT:PSS system. First, we suggest that current in PEDOT:PSS is transported in quasi-1D PEDOT-rich filaments which are embedded in a PSS-rich matrix, as indicated by the thick green and thin blue lines in **Figure 6**a. Along these filaments charges hop from site to site; such sites are shown in the zoom-in accented by the red square. Although PEDOT-rich grains are commonly observed in PEDOT:PSS, investigations of our PEDOT:PSS layers using AFM and STM could not reveal evidence for such grains.[8,18,19] Therefore we do not claim that hopping takes place between grains; e.g., the hopping sites might also be single or aggregated PEDOT oligomers along an extended PSS chain. The sites among which the hopping takes place are however restricted to filaments. Second, filaments that participate in conduction need to be part of a percolating network which connects to both electrodes. In Figure 6a these filaments are drawn as thick green lines. We suggest that the conductivity of this network is determined by the conductivity of the filaments as opposed to the connections between the filaments. This way the temperature and field dependence of the conductivity is that of the intra-filament conductivity. The resulting network can be approximated as a large set of parallel filaments. Such sets are known to show VRH-type behavior with a characteristic exponent of $\alpha = 1/2$.[31,32,33,47] Reduction of the PEDOT:PSS ratio by addition of the insulating PSS decreases the density of the PEDOT-rich filaments. This way, the conducting network is diluted and consequentially the probability for a filament to participate in the conducting network decreases. According to percolation theory, this gives rise to the observed power law dependence of the conductivity on the concentration of conductive material, provided the network is sufficiently close to the percolation threshold.[41]

The dependence of T_0 on PEDOT concentration and the observation that the measured values of α are somewhat below $\alpha = 1/2$, can be explained by the corrections for finite filament lengths by Raikh and Ruzin[47] to Mott's quasi-1D VRH.

Filaments with finite lengths can still be described by Equation (1) using a corrected characteristic temperature $T^*(L_{fil},T)$ which depends on temperature, causing $\alpha < 1/2$. Additionally since at higher PEDOT concentrations there are more connections between filaments, the length of the filaments between connections becomes shorter, therefore the dependence of T^* on filament length, L_{fil}, causes the trend in T_0 with PEDOT concentration.

2.4. Characterization of the Field Dependence of the Conductivity of Native Processed PEDOT:PSS Films as a Function of the PEDOT to PSS Ratio

To obtain further information about the characteristics of the conducting network, the field dependence in Figure 2 has been analyzed. Pollak and Riess[48] predict for non-Ohmic transport in variable range hopping systems:

$$\sigma(F,T) \propto \exp\left(a\frac{eFL(T)}{k_BT}\right) \quad (2)$$

where F denotes the electric field, e the electron charge, $L(T)$ the effective length of a hop, a is a constant related to the angle between the hopping direction and the field and k_B denotes the Boltzmann constant. For anisotropic systems, like PEDOT:PSS, the value of a may differ slightly from the value $a = 0.17$ for an isotropic system that was used here in order to limit the number of free parameters. Expression (2) is valid in the intermediate field range, i.e., where $(T_0/T)^{\alpha}k_BT > eFL(T) > k_BT$. Therefore fits in Figure 2 are restricted to $1.3 < \sigma(F,T)/\sigma_{OHM}(T) < 2$, i.e., the points indicated by the circular markers. The low temperature non-Ohmic curves in Figure 2 show that the intermediate field regime relates to a bending point in log σ vs. F, so that even though Equation (2) does not describe the whole curve, $L(T)$ is uniquely defined. Equation (2) has been derived for 2D and 3D variable range hopping and takes into account the effect of a change in the percolating path due to the field. In the thin films discussed in this study we expect the network of quasi-1D filaments to extend in three dimensions, where the finite thickness might affect the value of c in Equation (2). Numerical simulations of quasi-1D VRH systems support the use of Equation (2) for these systems.[33]

The effective hopping lengths, derived from Equation (2), determined for native processed PEDOT:PSS films in ratio 1:6 are shown in **Figure 7**. Similar graphs for other ratios are shown in the Supporting Information (Figure S2). In Figure 7 the filled red symbols indicate results obtained using Equation (2) directly to available data in the intermediate field regime. Since at high temperatures experimental conditions did not allow to reach these fields, an empirical extrapolation has been used, as discussed in the Supporting Information. The open blue symbols show the effective hopping lengths obtained by this procedure.

The magnitude of the typical length-scale L is, for all temperatures, compatible with the length of the filamentary structures observed in TEM and decreases with increasing temperature. In variable range hopping this occurs because at lower temperatures the lower thermal energy restricts the hopping to sites

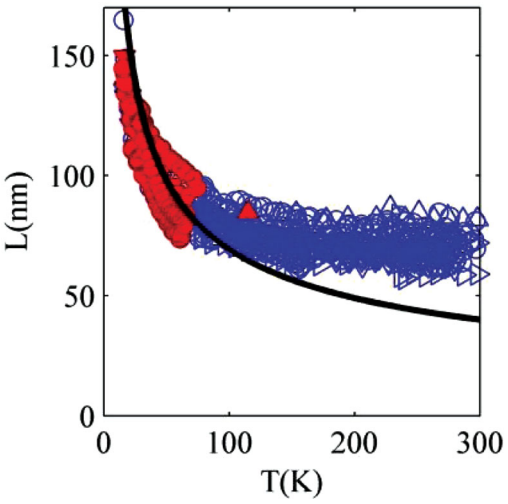

Figure 7. Extracted effective hopping lengths from *I–V* measurements on PEDOT:PSS films with ratio 1:6. The solid red symbols represent fits of Equation (2) to data in the intermediate field range. The open blue symbols represent extrapolated values based on the Ohmic and low field ranges. To correct for temperature inaccuracies at low temperatures the temperature was determined by the Ohmic conductivity using Equation (1) and $\alpha = 1/2$. The thick black line represents expected results based on Equation (3) for a localization length $\xi = 10$ nm in quasi-1D.

with energies closer to the Fermi level. This restriction forces the charge carriers to make longer hops, as described by:[34]

$$L(T) = c_L\xi\left(\frac{T_0}{T}\right)^{\alpha} \quad (3)$$

where c_L is a constant depending on the dimensionality of the system, for quasi-1D[33] $c_L = 2.6$, and ξ is the localization length. The hopping rate between two states decays exponentially with the distance, with a decay length $\xi/2$. The black line in Figure 7 shows that the predicted effective hopping lengths are consistent with an effective localization length of $\xi = 10$ nm. The same effective localization length gives a good description for all PEDOT:PSS ratios, with the exception of PEDOT:PSS in the ratio 1:2.5, which deviates slightly. This is most probably caused by heating of the layer during high voltage pulses. A quantitative analysis of such heating is presented in the Supporting Information.

Three other studies were able to provide estimates for the effective localization length in PEDOT: a similar layer approach on a different layer yielded $\xi = 8.2$ nm,[9] a study into the electrical properties of single PEDOT:PSS nanowires found $\xi = 0.07$ nm,[4,49] and measurements probing the magnetoresistance of PEDOT:PSS thin films led to $\xi = 10$ nm.[26] The effective localization length determined here is larger than the typical exponential wave-function decay of a molecular orbital.[38] This can be explained by a rescaling of the field due to metallic regions,[9,38] the finite macroscopic length scale for percolation,[38,50] or the presence of a band close to the Fermi level.[38] In either case, we conclude that the measured field dependent in-plane conductivity is well described by a percolating network of quasi-1D filaments, both qualitatively, i.e., the shapes of

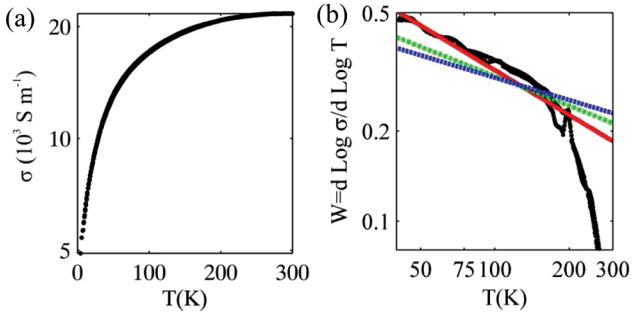

Figure 8. Measured a) Ohmic in-plane conductivity vs. temperature and b) the reduced activation energy *W* vs. temperature for PEDOT:PSS processed with HBS in the ratio 1:6. The red, green and blue lines indicate slopes of 1/2, 1/3 and 1/4, respectively. The black lines are double lines since the conductivity was measured while cooling down and while heating up.

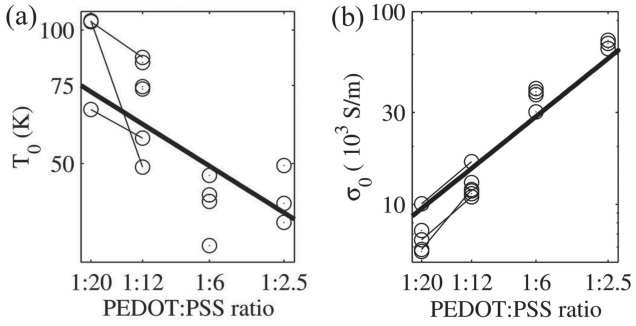

Figure 9. a) Characteristic temperatures and b) conductivity prefactors obtained from fits to the measured Ohmic conductivity vs. temperature for two spin coated samples for all four PEDOT:PSS ratios processed with HBS. Simultaneously measured data are connected by thin lines. Both panels are double-logarithmic plots with the x-axis scaled as the PEDOT concentration. The thick black line indicates a slope of a) −0.35 and b) 1.

$\sigma(V,T)$ and $L(T)$, and quantitatively, i.e., the determined localization length is in agreement with most published results.

2.5. Composition Dependence of the Conductivity of PEDOT:PSS Films Processed with High-Boiling Solvent

The in-plane conductivity of PEDOT:PSS films when processed with a high-boiling solvent (HBS) added to the PEDOT:PSS dispersion in water is much higher and has a much weaker temperature dependence than its native counterpart processed without HBS.[6,7,15,19,22,24,26] **Figure 8**a shows the conductivity as a function temperature for PEDOT:PSS processed with HBS with PEDOT:PSS ratio 1:6. To study the behavior of the Ohmic conductivity as a function of temperature we calculated the reduced activation energy *W* for this measurement, as is shown in Figure 8b. Similar graphs for the other ratios are shown in the Supporting Information as Figure S3. For each curve, fits to Equation (1) are added for values of $\alpha = 1/2$, 1/3, and 1/4 which are, successively, the red, green, and blue curves. The fit parameters for the fits for $\alpha = 1/2$ are shown in Table 1 as these give the best representation of the data below ≈200 K suggesting quasi-1D VRH behavior as was found for the PEDOT:PSS films processed without HBS.[15,19,22,26] Deviations from VRH-type conductivity above ≈200 K are discussed below.

Figure 9a shows the T_0 values obtained for the fits with $\alpha = 1/2$ for several measurements of two sets of spin coated samples. Extracted values of T_0 range from 30 to 100 K, which is lower than the lowest $T_0 \approx 275$ K found for PEDOT:PSS processed with a HBS in literature.[26] Other references[15,19,22] show $T_0 > \approx 1000$ K. These differences likely relate to the different PEDOT:PSS materials used. As in the PEDOT:PSS processed without HBS, a trend of decreasing T_0 with increasing c_{PEDOT} can be observed, which can be described as $T_0 \propto c^{-0.35}_{PEDOT}$, as indicated by the black line. Again, connections are shown between data points which have been obtained in simultaneous measurements, confirming this trend. Figure 9b shows the conductivity prefactor for the same samples. The conductivity prefactor shows an increasing trend with c_{PEDOT} which can be described as $\sigma_0 \propto c^{1}_{PEDOT}$, as indicated by the black line. The weak dependence of the conductivity prefactor on the PEDOT:PSS ratio suggests that the system is no longer close to the percolation threshold where power law behavior is observed; cf. Figure 4. Rather, the linear dependence on concentration suggests a well-connected system, far beyond the percolation threshold. In this regime, the material conductivity becomes linearly proportional to the fraction of conductive material.

Conductivity enhancement in PEDOT:PSS due to processing with HBS has been extensively studied, resulting in several explanatory schemes. Many authors[22,23,25,26] find evidence that HBS induce a phase segregation between PEDOT:PSS and PSSH, i.e., PSS which is not bound to PEDOT. This way, PSS barriers in the PEDOT-rich phase are reduced. Other schemes to explain the conductivity changes upon processing with HBS, which are sometimes used in combination, include conformational changes of PEDOT:PSS toward linear structures,[15,19,22,24,25] the influence of screening by the polar character of the HBS,[6,15,22,24] a change from polaron to bipolaron conduction[15] and increased inter-chain coupling.[7]

Interpretation of the conduction mechanism is difficult because of the weak temperature dependence of the conductivity in Figure 8, reflected in the low values for T_0 in Figure 9a. Interpretation in terms of quasi-1D VRH behavior, as for the formulations without HBS, is awkward since the observed $(T_0/T)^{0.5} = 0.4–1.2$ is inconsistent with the requirement $(T_0/T)^{0.5} >> 1$. In studies of PEDOT:PSS processed with HBS where the conductivity can no longer be correctly described by quasi-1D VRH, the change in conduction behavior is often described in the context of a metal-insulator transition.[6,7,26] In this scenario the quantum mechanical overlap between sites originally involved in Mott VRH increases beyond the point where charges can be treated as being localized on a specific site. This causes a change in conduction behavior from VRH to the critical regime where $\sigma(T) \propto T^{\beta}$ with $\beta = 0.3–1$,[51] for which the reduced activation energy is constant: $W = \beta$. Although Figure 8 does not show temperature independent reduced activation energies, the extracted values do match the expected values for β in the critical regime. We therefore tentatively conclude that we are in the crossover between quasi-1D

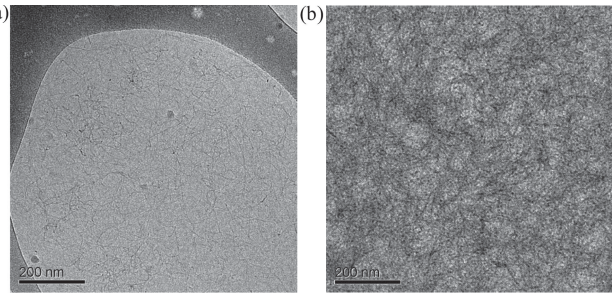

Figure 10. a) Cryo-TEM image of PEDOT:PSS dispersion with HBS in the ratio 1:2.5. The darker area is the TEM grid. The typical diameter of the filaments is 4–5 nm and their length may reach tens to hundreds of nanometers. b) HRTEM image of a dry specimen prepared from the same sample. The filaments look denser, and their diameter is smaller.

VRH and the critical regime, where characteristics of VRH are still dominant. As VRH is a low temperature phenomenon the deviations from VRH behavior are expected to predominantly arise at higher temperatures, in agreement with our observations.

Figure 10a,b shows TEM images of vitrified dispersions (cryo-TEM) and dried layers (HRTEM) of PEDOT:PSS samples processed with HBS. In surprising similarity to native processed PEDOT:PSS, these are dominated by the presence of randomly oriented worm-like filaments. This similarity in morphology implies that processing with HBS changes the resulting PEDOT:PSS in a subtle way that cannot be resolved by TEM.

Recently, Yeo et al. showed that the suggested phase segregation between PEDOT-rich and PSSH-rich regions occurs in the vertical direction with the PSSH on top.[10] Such a vertical phase segregation would both cause an increase in conductivity and be difficult to observe in TEM. However, simply extrapolating the results for native processed PEDOT:PSS according to the increased PEDOT:PSS ratio in the PEDOT-rich regions cannot explain the orders of magnitude increase in conductivity upon processing with HBS.[52] Instead, it is likely that processing with HBS causes a larger part of the filaments to contribute to the conduction. This will shift the network away from the percolation threshold, rationalizing the fact that the conductivity becomes linearly proportional to the PEDOT concentration. A schematic representation of this is given in Figure 6. This explanation requires that in the native processed PEDOT:PSS only a small fraction of the filaments takes part in conduction. This, in turn, resolves the seeming contradiction between the observation by TEM of a very dense filamentary network in dried layers of native processed PEDOT:PSS, and the dilute network with a typical length scale of ~100 nm evoked in the discussion of the conductivity: if all of the filaments observed in HRTEM would take part in conduction, the argument for the observed percolation behavior for native processed PEDOT:PSS would fail.

It is difficult to deduct from the data presented here the mechanism by which processing with HBS causes a larger part of the filaments to take part in conduction. Generally spoken this could be due to improved intra- and/or inter-filament transport. The former would imply that the HBS causes a strong reduction in the fraction of low-conductivity filaments, i.e., most filaments have become highly conductive and contribute to the conducting network. Alternatively, improved inter-filament transport would imply that the connectedness of the filaments is increased by the processing with HBS, as suggested in ref. [7]. Given the steep distance dependence of the tunneling rate between neighboring sites, small changes in the inter-filament distance could cause a much larger part of the filaments to participate in conductivity. Likewise, small changes in the intra-filament packing could dramatically improve intra-filament transport. Both mechanisms cannot be distinguished on basis of the present data and can be induced during annealing by the presence of HBS which favorably interacts with PEDOT. Importantly, both improved intra- and inter-filament transport will change the parameters σ_0 and T_0. For the enhanced intra-filament transport this is evident as σ_0 and T_0 both depend on the characteristic, most difficult hop in the network. However, this hop will also change when the density of connected filaments increases and their mean length decreases due to an enhanced filament connectivity.

3. Conclusions

The in-plane conductivity of PEDOT:PSS as a function of temperature, electric field, and PSS:PEDOT ratio has been systematically characterized for films that were processed with and without high boiling solvent (HBS).

The temperature dependence of the Ohmic conductivity for the PEDOT:PSS films processed without HBS is consistent with variable range hopping. By changing the PEDOT:PSS ratio we were able to show that the charge transport is governed by percolation. The critical concentration at which percolation sets in is low, suggesting that the percolating elements are strongly elongated. TEM images of both the dispersion and dried layers of PEDOT:PSS confirm the presence of filaments, which we propose to consist of a PEDOT-rich core with a PSS-rich shell. The percolating filament network can be regarded as a system of many quasi-1D wires in parallel, where the transport within the wires takes place by hopping, leading to quasi-1D VRH behavior.

Processing PEDOT:PSS with HBS does not cause significant changes in the morphology of the dried layers as evidenced by TEM, but the films exhibit a much higher in-plane conductivity. For temperatures below 200 K, the HBS-processed PDEOT:PSS films also show quasi-1D VRH behavior. However, the low characteristic temperature does not fully allow interpretation in terms of a VRH system and we propose that PEDOT:PSS processed with HBS is close to the critical regime between a metal and an insulator also because the conductivity prefactor shows a much weaker, linear dependence on the PEDOT concentration. This can be explained by a larger number of filaments participating in conduction after HBS treatment, either because of a smaller spread in (enhanced) filament conductivity or because of a larger probability for neighboring filaments to be connected.

4. Experimental Section

Sample Preparation: PEDOT:PSS dispersions were obtained from AGFA-Gevaert N.V. The dispersion used to prepare the samples is PEDOT:PSS ratio 1:2.5, which is commercially available without HBS

as Orgacon ICP-1050 and with HBS as Orgacon HIL-1005. PEDOT:PSS ratios 1:2.5, 1:6, 1:12, 1:20, were prepared using the stock dispersion of PEDOT:PSS in ratio 1:2.5 with and without HBS. The PEDOT:PSS ratio was adapted using the PSS stock dispersion used during the polymerization of the PEDOT. Where necessary, water was added to obtain a PEDOT:PSS solid content of (0.90 ± 0.04) wt%. This was followed by sonication to obtain homogeneous dispersions.

Samples for electrical measurements were prepared as follows, i.e., similar to ref. [9]: The substrates consisted of 3 cm × 3 cm bare sodalime glass. They were first grooved into small pieces of 1 cm × 1 cm on the back side with a diamond pen, then sonicated in a bath of acetone for 10 min, cleaned with soap, rinsed with deionized water for 20 min and sonicated in a bath of isopropanol for 10 min. Residual organic contaminations were removed using a 30 min. UV-ozone treatment (UV-Ozone Photoreactor, PR-100, Ultraviolet Products).

The PEDOT:PSS dispersions were filtered using a 0.5 µm filter and deposited in air by spin coating at 1000 RPM for 1 min, followed by 3000 RPM for 1 min to dry the layer. This typically resulted in layer thicknesses of 60 nm, 45 nm, 40 nm and 30 nm for native (without HBS) PEDOT:PSS in ratio of 1:2.5, 1:6, 1:12 and 1:20 respectively and in layer thicknesses of 70 nm, 55 nm, 55 nm and 50 nm for PEDOT:PSS processed with HBS in ratio of 1:2.5, 1:6, 1:12 and 1:20 respectively. After spin coating, samples were transferred into a glove box (O_2 and H_2O < 1 ppm) and subsequently annealed on a hot plate at 200 °C for a few minutes to remove residual water. Four electrodes (1 mm × 8 mm, 1 mm apart from each other) of 100 nm of gold were evaporated on top of each 1 cm × 1 cm piece.

After breaking the desired sample from the substrate, it was placed inside a cryostat (Oxford Instruments, modified for reaching low pressures) and evacuated to pressures below 10^{-6} mbar. The samples were exposed to air for a few minutes between the removal from the glove box and insertion into the cryostat. It was found that the room temperature conductivity only changes after exposure to air for a few hours. Once placed, samples were degassed at 200 °C for a few hours to reach low pressures. This annealing step in vacuum did not alter the room temperature conductivity.

Electrical Characterization: Conductivity measurements were performed using a Keithley 2636a low current source-measure unit. The Ohmic conductivity was sampled continuously at 200 mV while the temperature was ramped at a rate of 1 K min^{-1}. The temperature ramping was interrupted for measurements of the non-Ohmic conductivity, which were performed at constant temperature after settling for 5 min. For samples with high conductivity and at high voltages, pulsed measurements and modeling of the temperature during the pulses were necessary to obtain reliable data as discussed in the Supporting Information. Long continuous measurements of ≈24 h were made possible using a LABVIEW control program. Temperature control was provided by an Oxford ITC 601 temperature controller that maintained temperature stability within ±0.1 K. Measurements were performed in the range 4–300 K, where the minimum temperature was limited by the finite thermal contact with the cold finger and the maximum temperature was chosen to prevent ionic currents which can deteriorate the samples. The thermometer of the Oxford ITC 601 is used for all measurements presented here. To estimate the uncertainty in the obtained temperature measurements, calibration measurements using an additional thermometer were performed. The additional thermometer was located on the cold finger on which also the sample was mounted. This measurement showed that the temperature difference between the additional thermometer and the temperature determined using the temperature controller was at most 2.5 K and occurred below 70 K. Above 70 K the temperature difference was at most 1 K.

Transmission Electron Microscopy at Cryogenic Temperatures (Cryo-TEM) and High Resolution TEM (HRTEM): Samples for cryo-TEM imaging were prepared by depositing a droplet of typically 5 µL on perforated polymer film supported on a 300 mesh carbon coated electron microscope grid (copper, Ted Pella - lacey substrate). Ultra-thin films (10–250 nm) were formed as most of the dispersion was removed by blotting. The process was carried out in a controlled environment vitrification system where the temperature and the relative humidity are controlled, using an automatic Plunger- Freezer system by Leica (EM GP). The samples were examined at –178 °C using a FEI Tecnai 12 G^2 TWIN TEM equipped with a Gatan 626 cold stage. Samples for HRTEM imaging were prepared by placing a droplet of the dispersion on a TEM grid (300 mesh Cu, Ted Pella Ltd.) and allowing the solvent to evaporate.

Supporting Information

Supporting Information is available from the Wiley Online Library or from the author.

Acknowledgements

The authors wish to thank Paul van der Schoot for informative discussions, Yael Kalisman and Einat Nativ-Roth for support with the TEM experiments, Marco van der Sluis, Sandra Kouijzer and Veronique Gevaerts for their assistance with experiments, and Zuhal Tasdemir for performing experiments during the early stages of this research.

Received: April 5, 2013
Published online: June 19, 2013

[1] Y. H. Kim, C. Sachse, M. L. Machala, C. May, L. Müller-Meskamp, K. Leo, *Adv. Funct. Mater* **2011**, *21*, 1076.
[2] Y. Xia, K. Sun, J. Ouyang, *Adv. Mater.* **2012**, *24*, 2436.
[3] A. Aleshin, R. Kiebooms, R. Menon, A. J. Heeger, *Synth. Met.* **1997**, *90*, 61.
[4] Y. Cao, A. E. Kovalev, R. Xiao, J. Kim, T. S. Mayer, T. E. Mallouk, *Nano Lett.* **2008**, *8*, 4653.
[5] J. L. Duvail, P. Rétho, V. Fernandez, G. Louarn, P. Molinié, O. Chauvet, *J. Phys. Chem. B* **2004**, *108*, 18552.
[6] J. Y. Kim, J. H. Jung, D. E. Lee, J. Joo, *Synth. Met.* **2002**, *126*, 311.
[7] N. Kim, B. H. Lee, D. Choi, G. Kim, H. Kim, J.-R. Kim, J. Lee, Y. H. Kahng, K. Lee, *Phys. Rev. Lett.* **2012**, *109*, 106405.
[8] A. M. Nardes, M. Kemerink, R. A. J. Janssen, J. A. M. Bastiaansen, N. M. M. Kiggen, B. M. W. Langeveld, A. J. J. M. van Breemen, M. M. de Kok, *Adv. Mater.* **2007**, *19*, 1196.
[9] A. M. Nardes, M. Kemerink, R. A. J. Janssen, *Phys. Rev. B* **2007**, *76*, 085208.
[10] J.-S. Yeo, J.-M. Yun, D.-Y. Kim, S. Park, S.-S. Kim, M.-H. Yoon, T.-W. Kim, S.-I. Na, *ACS Appl. Mater. Interfaces* **2012**, *4*, 2551.
[11] A. J. Kronemeijer, E. H. Huisman, I. Katsouras, P. A. van Hal, T. C. T. Geuns, P. W. M. Blom, S. J. van der Molen, D. M. de Leeuw, *Phys. Rev. Lett.* **2010**, *105*, 156604.
[12] I. Katsouras, A. J. Kronemeijer, E. C. P. Smits, P. A. van Hal, T. C. T. Geuns, P. W. M. Blom, D. M. de Leeuw, *Appl. Phys. Lett.* **2011**, *99*, 013303.
[13] O. Bubnova, Z. U. Khan, A. Malti, S. Braun, M. Fahlman, M. Berggren, X. Crispin, *Nat. Mater.* **2011**, *10*, 429.
[14] D. S. H. Charrier, R. A. J. Janssen, M. Kemerink, *Chem. Mater.* **2010**, *22*, 3670.
[15] J. Ouyang, Q. Xu, C.-W. Chu, Y. Yang, G. Li, J. Shinar, *Polymer* **2004**, *45*, 8443.
[16] T. Takano, H. Masunaga, A. Fujiwara, H. Okuzaki, T. Sasaki, *Macromolecules* **2012**, *45*, 3859.
[17] G. Greczynski, T. Kugler, M. Keil, W. Osikowicz, M. Fahlman, W. Salaneck, *J. Electron. Spectrosc. Relat. Phenom* **2001**, *121*, 1.
[18] U. Lang, E. Müller, N. Naujoks, J. Dual, *Adv. Funct. Mater.* **2009**, *19*, 1215.

[19] A. M. Nardes, R. A. J. Janssen, M. Kemerink, *Adv. Funct. Mater.* **2008**, *18*, 865.
[20] J. Hwang, F. Amy, A. Kahn, *Org. Electron.* **2006**, *7*, 387.
[21] C. Ionescu-Zanetti, A. Mechler, S. A. Carter, R. Lal, *Adv. Mater.* **2004**, *16*, 385.
[22] Y. Xia, J. Ouyang, *J. Mater. Chem.* **2011**, *21*, 4927.
[23] X. Crispin, F. L. E. Jakobsson, A. Crispin, P. C. M. Grim, P. Andersson, A. Volodin, C. van Haesendonck, M. Van der Auweraer, W. R. Salaneck, M. Berggren, *Chem. Mater.* **2006**, *18*, 4354.
[24] H. Okuzaki, Y. Harashina, H. Yan, *Eur. Polym. J.* **2009**, *45*, 256.
[25] T. Wang, Y. Qi, J. Xu, X. Hu, P. Chen, *Appl. Surf. Sci.* **2005**, *250*, 188.
[26] C. S. Suchand Sangeeth, M. Jaiswal, R. Menon, *J. Phys.: Condens. Matter* **2009**, *21*, 072101.
[27] S. Samitsu, T. Shimomura, K. Ito, M. Fujimori, S. Heike, T. Hashizume, *Appl. Phys. Lett.* **2005**, *86*, 233103.
[28] A. N. Aleshin, S. R. Williams, A. J. Heeger, *Synth. Met.* **1998**, *94*, 173.
[29] J. Joo, S. M. Long, J. P. Pouget, E. J. Oh, A. G. MacDiarmid, A. J. Epstein, *Phys. Rev. B* **1998**, *57*, 9567.
[30] E. Abrahams, P. W. Anderson, D. C. Licciardello, T. V. Ramakrishnan, *Phys. Rev. Lett.* **1979**, *42*, 673.
[31] A. S. Rodin, M. M. Fogler, *Phys. Rev. Lett.* **2010**, *105*, 106801.
[32] K. Maschke, H. Overhof, P. Thomas, *Phys. Stat. Solidi B* **1974**, *61*, 621.
[33] A. S. Rodin, M. M. Fogler, *Phys. Rev. B* **2009**, *80*, 155435.
[34] B. I. Shklovskii, A. L. Efros, *Electronic Properties of Doped Semiconductors*, Springer-Verlag, Berlin **1984**.
[35] Not all references shown explicitly mention values of T_0, in those cases we have extracted T_0 from figures of the data.
[36] C. L. Pint, Y.-Q. Xu, E. Morosan, R. H. Hauge, *Appl. Phys. Lett.* **2009**, *94*, 182107.
[37] F. J. Rueß, A. P. Micolich, W. Pok, K. E. J. Goh, A. R. Hamilton, M. Y. Simmons, *Appl. Phys. Lett.* **2008**, *92*, 052101.
[38] For a more elaborate discussion, see the Supporting Information.
[39] P. Sheng, B. Abeles, Y. Arie, *Phys. Rev. Lett.* **1973**, *31*, 44.
[40] L. Zuppiroli, M. N. Bussac, S. Paschen, O. Chauvet, L. Forro, *Phys. Rev. B* **1994**, *50*, 5196.
[41] Y. P. Mamunya, *J. Macromol. Sci. B* **1999**, *38*, 615.
[42] C. D. Lorenz, R. M. Ziff, *J. Chem. Phys.* **2001**, *114*, 3659.
[43] Y. B. Yi, E. Tawerghi, *Phys. Rev. E* **2009**, *79*, 041134.
[44] M. Foygel, R. D. Morris, D. Anez, S. French, V. L. Sobolev, *Phys. Rev. B* **2005**, *71*, 104201.
[45] G. Zotti, S. Zecchin, G. Schiavon, F. Louwet, L. Groenendaal, X. Crispin, W. Osikowicz, W. Salaneck, M. Fahlman, *Macromolecules* **2003**, *36*, 3337.
[46] B. Friedel, T. J. K. Brenner, C. R. McNeill, U. Steiner, N. C. Greenham, *Org. Electron.* **2011**, *12*, 1736.
[47] M. E. Raikh, I. M. Ruzin, *Sov. Phys. JETP* **1989**, *68*, 642.
[48] M. Pollak, I. Riess, *J. Phys. C* **1976**, *9*, 2339.
[49] In Reference [4] using the slope in Figure 4 and Equation (2) presented here, it can be determined that $L = 1.2$ nm at 10 K. Using Equation (3) this results in $\xi = 0.07$ nm.
[50] B. I. Shklovskii, *Sov. Phys. Semicond.* **1977**, *10*, 855.
[51] A. I. Larkin, *Sov. Phys. JETP* **1982**, *56*, 647.
[52] Increasing the conductivity from $\sigma_0 = 1.8\ 10^3$ S m^{-1} for native PEDOT:PSS in the ratio 1:2.5 to $\sigma_0 = 6.3\ 10^4$ S m^{-1} for PEDOT:PSS in the ratio 2:5 with HBS requires according to $\sigma_0 \propto c_{\mathrm{PEDOT}}^{3.5}$ an effective PEDOT:PSS ratio of 4:1 at the bottom of the PEDOT:PSS layer, which is unlikely high.